

Crystal Phase of Poly(vinylidene fluoride-co-trifluoroethylene) Synthesized via Hydrogenation of Poly(vinylidene fluoride-co-chlorotrifluoroethylene)

Qiuping Zhang,¹ Weimin Xia,² Zhigang Zhu,¹ Zhicheng Zhang^{1,3}

¹Department of Applied Chemistry, School of Science, Xi'an Jiaotong University, Xi'an 710049, People's Republic of China

²Electronic Materials Research Laboratory, Key Laboratory of the Ministry of Education & International Center for Dielectric Research, Xi'an Jiaotong University, Xi'an 710049, People's Republic of China

³MOE Key Laboratory for Nonequilibrium Synthesis and Modulation of Condensed Matter, Xi'an Jiaotong University, Xi'an 710049, People's Republic of China

Correspondence to: Z. Zhang (E-mail: zhichengzhang@mail.xjtu.edu.cn)

ABSTRACT: Trifluoroethylene addition and thermal treatment induced crystal phase transition in a series of poly(vinylidene fluoride-co-trifluoroethylene) [P(VDF-co-TrFE)] containing varied TrFE molar ratio (6, 9, 12, and 20 mol %) prepared from the hydrogenation of poly(vinylidene fluoride-co-chlorotrifluoroethylene) have been investigated by means of Fourier transform infrared spectral (FTIR), X-ray diffraction (XRD), and differential scanning calorimetry (DSC) analyses. The comprehensive applications of the three techniques could distinguish α , β and γ phase of P(VDF-co-TrFE) very well. The multipeak fitting technique of DSC is successfully applied to calculate the percentage of different phases in the samples, which allows us to investigate the phase transition process of P(VDF-co-TrFE) precisely. It is found that the crystal phase of P(VDF-co-TrFE) films is turned from $\alpha + \gamma$ phase (6 mol % TrFE) to $\alpha + \gamma + \beta$ phase (9 and 12 mol % TrFE) to β phase (20 mol % TrFE) at high temperature, and from $\alpha + \gamma$ phase (6 mol % TrFE) to $\gamma + \beta$ phase (9 mol % TrFE) to β phase (>12 mol % TrFE) at low fabricated temperature. Both the fabrication conditions and TrFE addition are responsible for the crystal phase transition of the hydrogenised P(VDF-co-TrFE). © 2012 Wiley Periodicals, Inc. *J. Appl. Polym. Sci.* 000: 000–000, 2012

KEYWORDS: P(VDF-co-TrFE); FTIR; XRD; DSC; phase transition

Received 22 February 2012; accepted 27 April 2012; published online

DOI: 10.1002/app.37975

INTRODUCTION

Since the initial study about the strong piezoelectricity and pyroelectricity properties of poly(vinylidene fluoride) (PVDF) and its copolymer poly(vinylidene fluoride-co-trifluoroethylene) [P(VDF-co-TrFE)] in the 1970s,^{1–4} PVDF and P(VDF-co-TrFE) have attracted considerable interests for their various device applications such as electromechanical sensors and actuators.⁵ Several years later, excellent ferroelectricity was disclosed in P(VDF-co-TrFE) by the existence of a Curie temperature at which the crystals undergo a ferroelectric-to-paraelectric phase transition in a wide range of the VDF composition ratio.^{6–13} The piezoelectricity, pyroelectricity, and ferroelectricity properties of these polymers are reported to be closely related to their molecular conformation and chain packing in crystals.

It has been well known that PVDF homopolymer could crystallize into at least four distinct phases including α phase [in

trans-gauche conformation (TG TG'), β phase [in all-*trans* planar zigzag conformation (TTTT)], γ phase [in a conformation of three *trans* linked to one *gauche* (TTTG)], and δ phase (in a polar version of α phase) depending on the fabrication conditions.¹⁴ The piezoelectricity, pyroelectricity, and ferroelectricity properties of PVDF are believed to be intimately related to the polar β crystalline phase. Typically, neat PVDF always has to go through mechanical stretching process or high temperature thermal treatment to induce the formation of β -phase.^{15,16} With the addition of over 17 mol% TrFE units via direct polymerization process, P(VDF-co-TrFE) chains prefer all-*trans* conformation and unit cell of β phase directly.¹⁷ Yagi et al.^{18–20} have investigated the molecule conformation and crystalline form of P(VDF-co-TrFE) over the entire range of composition by means of X-ray diffraction (XRD) and infrared spectroscopy. Pure PTrFE was found to be a stereo-irregular containing ~50% of inversely added monomeric units and adopt a 3/1-helical

© 2012 Wiley Periodicals, Inc.

conformation. The addition of less than about 85 mol % VDF could result in *trans* or *trans*-like conformation while higher VDF concentrations would yield TGTG' conformation in the copolymers.^{18–21} Mechanical stretching process, external electric-field polarization, and thermal treatment have been reported to exhibit significant influence on the final crystalline phases of these polymers as well.^{22–26}

In the previous investigation, Fourier transform infrared (or Raman spectra) and XRD have been the most frequently used tools to characterize the crystal phase and chain conformation of P(VDF-*co*-TrFE).^{10–13,27–31} However, as for the precise characterization of these three phases associated with the three basic conformations, divergent results are always obtained because neither the bands in FTIR spectra nor the diffraction reflection peaks in XRD spectra could be definitively assigned. Besides, compared with well-known α and β phases, γ phase associated with TTTG conformation has rarely been investigated because of the difficulty in the fabrication and characterization of pure γ phase. Meanwhile, the fact that conformation of both the β and γ phase has the TTT segments makes it even more difficult to distinguish γ from β phase. Differential scanning calorimeter (DSC) has also been applied in some work to study the crystal phase evolution of PVDF or P(VDF-*co*-TrFE).^{17,21,22,25,32–35} However, so far no method is able to precisely identify and calculate the exact percentage of the three crystal phases in the samples with more than one type of crystal phases.

Recently, the synthesis methodology of TrFE-containing PVDF-based fluoropolymer has undergone a rapid improvement along with the significant achievement obtained in PVDF-based ferroelectric relaxor as high electric energy storage dielectrics. For the disadvantages of TrFE as comonomer, such as the poor controllability of the copolymer composition due to varied reactivity ratios of different monomers, the difficulty during the transportation and storage of TrFE monomer, and the relatively poor sources of TrFE,³⁶ a more convenient chemical route, involving the copolymerization of VDF and chloridetrifluoro ethylene (CTFE) followed by the subsequent hydrogenation of P(VDF-*co*-CTFE) to convert CTFE units into TrFE units, is disclosed to synthesize TrFE-containing copolymers.³⁷ More recently, an environmentally friendly and controllable P(VDF-*co*-CTFE) hydrogenation route named atom transfer chain transfer reaction is reported by our group in an effort to avoid the use and production of high toxic chemicals (such as tributyltin hydride and tributyltin chloride).³⁸ Our previous study has demonstrated that VDF and TrFE units are mostly in head-head connection in the hydrogenated copolymer, which is responsible for the significant difference in the thermal and dielectric properties between the direct-copolymer and hydrogenized copolymer.³⁹ However, the systematic investigation of thermal treatment and composition influence on the crystalline properties of P(VDF-*co*-TrFE) with head-head VDF-TrFE connection are still unknown, although both the composition and the crystalline conditions are well recognized as dominate roles on the phase transition of P(VDF-*co*-TrFE).^{25,32} This promotes us to develop a more powerful and facile method, DSC peaks fitting technique combined with FTIR and XRD, to precisely evaluate how the composition and fabrication conditions affect the crystal phase

Table I. Fabrication Conditions of P(VDF-*co*-TrFE) Films with Different TrFE Molar Ratios

| Fabrication conditions | TrFE content (mol%) | | | |
|---|---------------------|----|----|----|
| | 6 | 9 | 12 | 20 |
| As-casted at 44°C | A1 | A2 | A3 | A4 |
| As-casted at 100°C | B1 | B2 | B3 | B4 |
| Annealed at 200°C | C1 | C2 | C3 | C4 |
| Quenched in ice-water | D1 | D2 | D3 | D4 |
| Quenched in N ₂ (l) + hexane | E1 | E2 | E3 | E4 |
| Quenched in liquid N ₂ (l) | F1 | F2 | F3 | F4 |

transition of indirectly polymerized P(VDF-*co*-TrFE) in this work.

EXPERIMENTAL SECTION

Materials

P(VDF-*co*-CTFE) containing varied CTFE molar ratio (6, 9, 12, and 20 mol %) was purchased from Solvay Solex and SynQuest Laboratory (America). All the other chemicals were obtained from commercials and used as received. P(VDF-*co*-TrFE)s with altered composition were synthesized by a full hydrogenation process of P(VDF-*co*-CTFE) following the procedure described in literature.³⁸ The structure of P(VDF-*co*-TrFE)s was confirmed by ¹H- and ¹⁹F-NMR.

Fabrication of P(VDF-*co*-TrFE) Films

The films about 10~20- μ m-thick were prepared *via* casting the polymer solution in dimethylformamide (DMF) onto glass substrate or a quartz slide. The subsequent thermal processing techniques were used as follows to fabricate six series corresponding samples with varied TrFE content as listed in Table I. A and B series samples are as-casted P(VDF-*co*-TrFE) films at 44 and 100°C, respectively, without any further thermal treatment. Films numbered from 1 to 4 correspond to the samples with TrFE molar content from 6 to 20 mol %. C series samples are annealed films prepared *via* heating the untreated film at 200°C for 4 h followed by cooling to ambient temperature gradually in 12 h. D, E, and F series samples are quenched films prepared *via* heating the as-casted films at 200°C for 4 h followed by immediately quenching into ice-water bath, hexane-liquid nitrogen bath, and liquid nitrogen, respectively.

Characterization

¹H- and ¹⁹F-NMR spectra were recorded on a Bruker (Advanced II) 400 MHz spectrometer instrument with acetone-*d*₆ as solvent and tetramethylsilane as an internal standard. DSC analysis was conducted on a NETZSCH DSC 200 PC (NETZSCH, Germany) in nitrogen atmosphere at a heating rate of 10, 5, or 2.5°C/min for the first circle. XRD results were obtained on a RIGAKU D/MAX-2400 (Rigaku Industrial, Japan). The wavelength of the X-ray was 1.542 Å (Cu K α radiation, 40 kV and 100 mA) and the scanning velocity was 4°/min. FTIR spectroscopy was carried out on a Tensor 27 (Bruker Corporation, Germany) with a resolution 1~0.4 cm⁻¹.

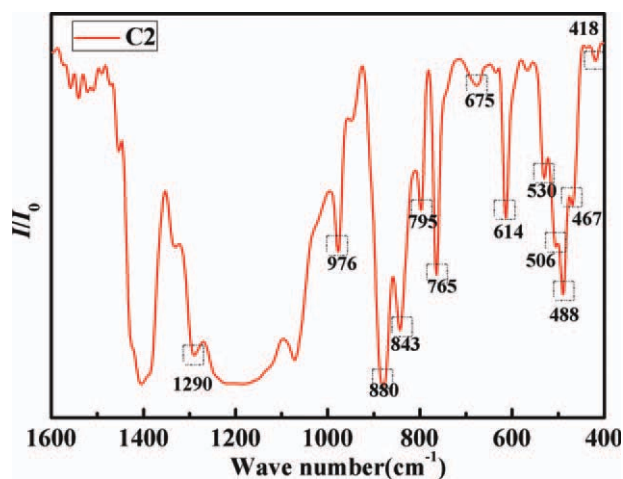


Figure 1. FTIR spectra of Sample C2 [9 mol % P(VDF-*co*-TrFE) film annealed at 200°C]. [Color figure can be viewed in the online issue, which is available at wileyonlinelibrary.com.]

RESULTS AND DISCUSSION

Characterization of P(VDF-*co*-TrFE) with Different Crystal Phases

FTIR and XRD are mostly used techniques to determine the crystalline structure and morphology as well as the conformation of the polymer chains in the crystalline regions of PVDF-based fluoropolymers.^{10–13,27–31} Comparing with neat PVDF, the introduction of TrFE makes the crystalline properties of resultant copolymer more complicated. It is well recognized that the FTIR absorbance peak at 1284–1290 cm^{-1} corresponds to the *trans* isomer sequence with four or more than four units (characteristic of β structure),^{9,10,16} the absorbance peak at 614 cm^{-1} is attributed to the *trans-gauche* sequence (TG) of α phase, and the band at 510 cm^{-1} is assigned to T₃G conformation⁷ corresponding to γ phase, respectively. Therefore, α phase could be clearly identified by the FTIR absorption bands at 530, 614, 765, 795, and 976 cm^{-1} . However, the identification of γ and β phases on FTIR is rather difficult for their similar polymer chain conformation and close characteristic absorption bands at 510, 810–840, and 1284–1290 cm^{-1} . As a matter of fact, none of these peaks could be applied to distinguish one type of crystal phase from the other one precisely, especially when the samples have the combined crystal phases. FTIR spectrum of sample C2, P(VDF-*co*-TrFE) film with 9 mol % TrFE is fabricated at 100°C and then cooled gradually after an isothermal at 200°C for 4 h, is presented as an example in Figure 1. The existence of α phase crystal could be clearly indentified by the sharp peak at 614 cm^{-1} , while the existence of γ or β could hardly be determined just by peaks at 510 and 1290 cm^{-1} .

XRD faces the similar problem as FTIR for the characterization of these three crystalline phases. It has been reported that the β crystalline phase in the semicrystalline P(VDF-*co*-TrFE) has an orthorhombic unit cell in which the lattice *a* and *b* axes are perpendicular to the polymer chain and their ratio is close to $\sqrt{3}$. Thus, the lattice has a quasi-hexagonal structure, resulting in the overlap of the (110) and (200) reflections.⁴⁰ The single reflection peak suited at $2\theta = 19.7^\circ$ is considered to be from

the ferroelectric β phase associated with the all-*trans* conformation and represents the Bragg diffraction of (110)/(200) of β phase. However, the Bragg diffraction of (110)/(200) of γ and α phases is very close at $2\theta = 20^\circ$ as well. Although $2\theta = 18.7^\circ$ is supposed to represent nonferroelectric phases, associated with α or γ phase, the reflection at $2\theta = 17.7^\circ$ and 26.8° are only from the Bragg diffractions of (100) and (021) of the nonpolar α phase, respectively.⁴¹ In other words, α phase of P(VDF-*co*-TrFE) of C2 (Figure 2) could be clearly identified on XRD spectra by Bragg diffractions at 17.7° and 26.8° , whereas β and γ phases could hardly be distinguished from Figure 2.

DSC curves of sample C2 at enhanced heating rate from 2.5 to 20°C/min is taken as an example as shown in Figure 3. Only two clear endothermic peaks are observed on the DSC curve obtained at the heating of 20°C/min. As the heating rate decreases from 20 to 2.5°C/min, the endothermic peak at 167.4°C is divided into two independent peaks at about 165 and 170°C gradually. Apparently, the original broad peak obtained at high heating rate is the combination of these two peaks. However, the low heating rate leads to the shifting of endothermic peak to lower temperature as well as lower fusion enthalpy. In order to separate the overlapped peaks obtained at the heating rate of 20°C/min, multipeak fitting technique has been used as shown in Figure 3. The magenta curves are corresponding to the fixed individual peaks, while the well coincided green line with the original DSC curve is the fitted results.

Our previous study has shown that the melting temperature of β phase is obviously lower than that of α and γ phase in neat PVDF, while the melting point of α -PVDF is slightly lower than γ -PVDF.⁴² Therefore, the three endothermic peaks observed in sample C2 at elevated temperature could be attributed to the melting temperature of β , α , and γ phases successively. That means the crystalline region of Sample C2 is composed of three mixed phases. Thus, DSC multipeak fitting technique could successfully distinguish the three crystalline phases from each other

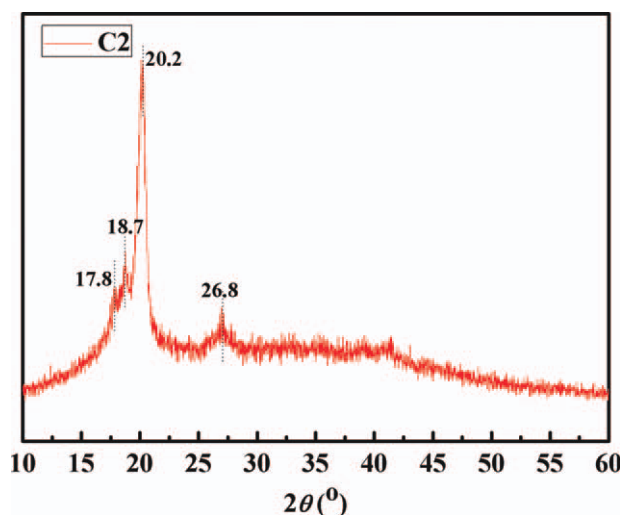


Figure 2. X-ray diffraction spectra of Sample C2 [9 mol % P(VDF-*co*-TrFE) film annealed at 200°C]. [Color figure can be viewed in the online issue, which is available at wileyonlinelibrary.com.]

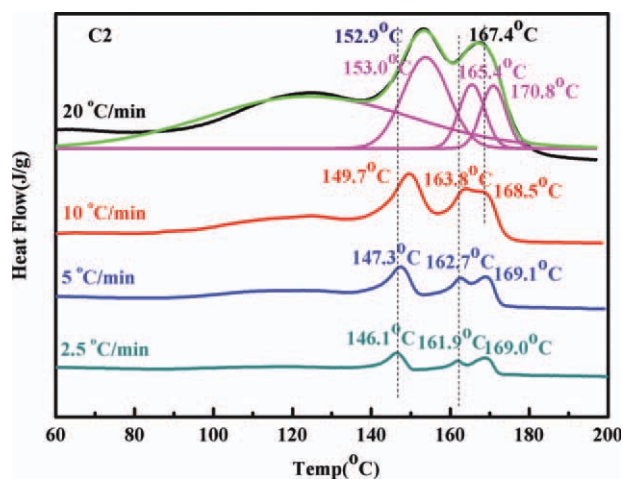


Figure 3. DSC of Sample C2 [9 mol % P(VDF-*co*-TrFE) film annealed at 200°C] obtained at elevated heating rate indicated by the numbers on the left side of the above picture. The result obtained at 20°C/min is fitted by the original multi-peaks fitting technique: the inner black curve comes from the original measured data. The green curve represents the fitting line while the magenta ones correspond to the separation results. [Color figure can be viewed in the online issue, which is available at wileyonlinelibrary.com.]

with the assistance of FTIR and XRD. Most importantly, the integral of the fixed individual peaks of DSC curve could help to estimate the percentage of each crystal phase in the samples possessing multicrystalline phases.

Phase Dependence of P(VDF-*co*-TrFE) on Fabrication Conditions

It has been well studied that the crystalline structure of PVDF-based semicrystalline polymers is strongly dependent on crystalline conditions, such as solvents and substrates utilized in solution cast process, crystalline temperature and thermal treatment.³² For example, thermal treatment, such as annealing at a temperature between the Curie temperature and melting point of P(VDF-*co*-TrFE), has been widely applied to fabricate films with improved ferroelectric phase.^{22,30,43,44} More interests have been focused on the ferroelectric-to-paraelectric (F-P) transition of copolymers rather than their crystalline phase transition,^{30,32,34,45} although their electric phase transition is very dependent on the crystal phase properties.

The IR spectra of P(VDF-*co*-TrFE) with 6 mol % TrFE thermally treated in different ways are shown in Figure 4. α phase in major could be observed in all the samples characterized with absorption bands at 530, 613, 764, 797, and 975 cm^{-1} . As the treatment temperature decreases, the characteristic absorption bands of α phase become sharper and more typical. The small peak at 511 cm^{-1} indicates the presence of β or γ phase. Figure 5 presents the XRD spectra of sample A1, B1, C1, D1, E1, and F1. B1, C1, D1, E1, and F1 all show Bragg diffraction at 17.7°, 18.7°, and 26.8°, indicating the existence of α phase. Instead, A1 has the Bragg diffraction at 18.7°, characteristic of nonferroelectric phase associated with α or γ phase.

DSC thermograms of these samples are shown in Figure 6. The peaks at 120~140°C are attributed to the well-known F-P

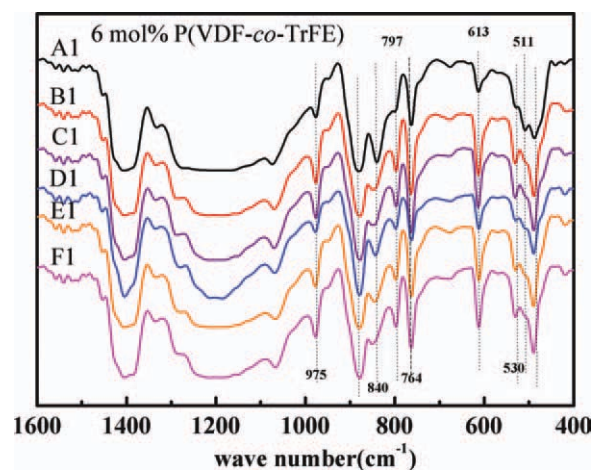


Figure 4. FTIR of P(VDF-*co*-TrFE) (6 mol % TrFE) films fabricated under various conditions: A1: as-casted at 44°C; B1: as-casted at 100°C; C1: annealed at 200°C; D1: quenched in ice-water; E1: quenched in $\text{N}_2(\text{l})$ +hexane; F1: quenched in liquid $\text{N}_2(\text{l})$. [Color figure can be viewed in the online issue, which is available at wileyonlinelibrary.com.]

transition or Curie temperature, which will not be discussed in this work. The broad melting peak of A1 could be separated into two endothermic peaks at 161.9 and 168.8°C with multi-peak fitting technique as discussed above, corresponding to the melting temperature of α and γ phases, respectively. The mixed crystalline phase characteristic of Sample B1 and C1 are much clearer with two obvious peaks, which are separated as well to investigate the percentage of each phase in the crystalline region. The peaks at 161.4°C of B1 and 163.1°C of C1 correspond to the melting point of α phase while the second peak at 168.4°C of B1 and 168.3°C of C1 corresponds to the melting point of γ

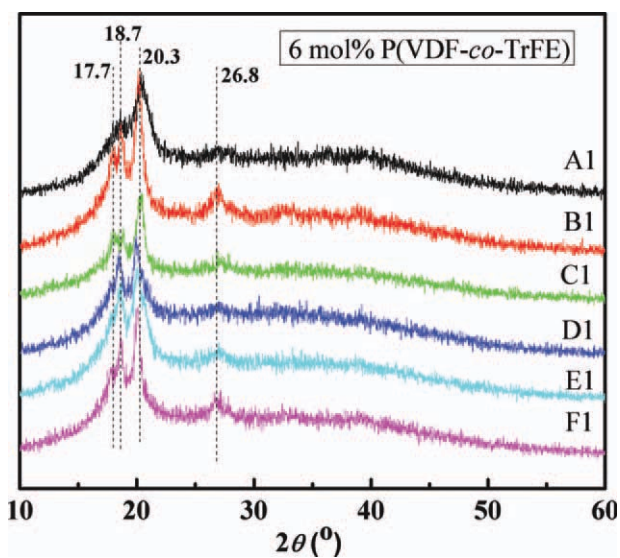


Figure 5. XRD of P(VDF-*co*-TrFE) (6 mol % TrFE) films fabricated under various conditions: A1: as-casted at 44°C; B1: as-casted at 100°C; C1: annealed at 200°C; D1: quenched in ice-water; E1: quenched in $\text{N}_2(\text{l})$ +hexane; F1: quenched in liquid $\text{N}_2(\text{l})$. [Color figure can be viewed in the online issue, which is available at wileyonlinelibrary.com.]

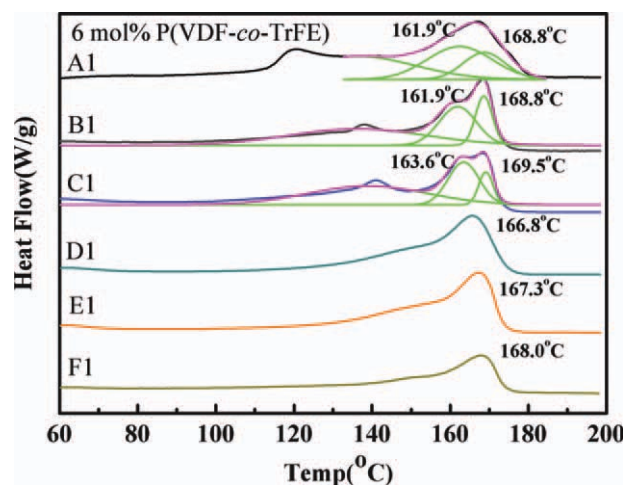


Figure 6. DSC of P(VDF-*co*-TrFE) (6 mol % TrFE) films fabricated under various conditions: A1: as-casted at 44°C; B1: as-casted at 100°C; C1: annealed at 200°C; D1: quenched in ice-water; E1: quenched in N₂(l) + hexane; F1: quenched in liquid N₂(l). [Color figure can be viewed in the online issue, which is available at wileyonlinelibrary.com.]

phase, which is consistent with results from FTIR and XRD. When the samples are quenched from high temperature immediately to low temperature, such as samples D1, E1, and F1, the two melting peaks are merged into one, corresponding to the contribution of α phase. In addition, the melting point shifts to higher temperature as the quenching temperature decreases, which may be caused by the increasing of gauche conformation, consistent with the results found by Farmer et al,⁴⁶ calculating the stability of *gauche* and *trans* conformation of VDF and tetrafluoroethylene (TFE) copolymer.

With the assistance of multipeak fitting technique, the percentage of each crystal phase in the overall crystalline region was calculated by dividing the melting fusion enthalpy of the individual melting peak with the overall fusion enthalpy as listed in Table II. It seems that γ phase with minor α phase is more likely to be formed in P(VDF-*co*-TrFE) containing 6 mol % TrFE fabricated at low temperature. The content of α phase increases as the fabrication temperature increases. Cooling from high temperature to low temperature favors the formation of α phase, and the higher cooling rate results in more α phase in crystal-

line region. As more TrFE introduced (>9 mol %), β phase starts to be determined. Films fabricated at low temperature favors the formation of crystal phase with higher polarity (γ or β phase) while high temperature leads to the various α phase content depending on the cooling rate. All the results coincide very well with the fact found in neat PVDF that high crystallization temperature favors the formation of kinetically favorable conformation (TGTG'), while the low crystallization temperature helps form TTTG conformation.⁴⁷

Phase Dependence of P(VDF-*co*-TrFE) on TrFE Content

It is well known that the crystal structure and phase transition of directly polymerized P(VDF-*co*-TrFE) depends strongly on VDF content. It has been reported that only *trans* conformation (β phase) could be observed in copolymer with more than 40 mol % TrFE regardless of the fabrication conditions. More or less *G* and *G'* conformation defects in major β phase are detected in the copolymer containing 18~40 mol % TrFE when it is cooled from high temperature to the temperature below T_c . Melt-crystallized copolymer with less than 18 mol % TrFE is found to contain α phase and possibly γ phase besides β phase in major.¹⁷ In order to investigate the exact crystal phase transition induced by TrFE of these P(VDF-*co*-TrFE) copolymers prepared in indirect polymerization process, annealed samples containing TrFE units no more than 20 mol % are taken as an instance for discussion.

As shown in Figure 7, the characteristic bands of α phase at 530, 614, 764, and 796 cm⁻¹ are fading while the absorption band of β or γ phase at 510 cm⁻¹ is growing as the TrFE content increases from 6 to 20 mol %. That means the introduction of more TrFE results in the crystal phase transition of the copolymer from α phase to β or γ phase. That confirms the result obtained in XRD as shown in Figure 8. The characteristic diffraction reflections of α and γ phases at $2\theta = 26.8^\circ$, 18.7° , and 17.8° on XRD reduce gradually with the increase of TrFE content, while the reflection at $2\theta = 20^\circ$ is growing and shifting from 20.3° of sample C1 to 19.5° of sample C4. That means the increasing TrFE content is responsible for the phase transition from α and γ phases to β phase.

DSC results of these four samples are shown in Figure 9. With the assistance of multipeak fitting technique, the phase transition induced by TrFE addition could be clearly identified. As TrFE content increases, the crystal phases of P(VDF-*co*-TrFE)

Table II. Content of Various Crystal phases in the Crystalline Region (%) Obtained in the Samples with Altered Compositions and Fabricated under Different Conditions

| Thermal treatment | Percentage of various crystal phases (%) | | | | | | | | | | | |
|-------------------|--|---------|----------|----------|---------|----------|----------|---------|----------|----------|---------|----------|
| | 94/6 | | | 91/9 | | | 88/12 | | | 80/20 | | |
| | α | β | γ | α | β | γ | α | β | γ | α | β | γ |
| A | 52.1 | 0 | 47.9 | 0 | 48.2 | 51.8 | 0 | 100 | 0 | 0 | 100 | 0 |
| B | 70.1 | 0 | 29.9 | 41.8 | 51.9 | 6.3 | 56.3 | 43.7 | 0 | 0 | 100 | 0 |
| C | 83.4 | 0 | 16.6 | 27.0 | 47.6 | 25.4 | 19.9 | 64.3 | 15.8 | 0 | 100 | 0 |
| D | 100 | 0 | 0 | 42.9 | 57.1 | 0 | 17.3 | 82.7 | 0 | 0 | 100 | 0 |
| E | 100 | 0 | 0 | 45.9 | 54.1 | 0 | 0 | 100 | 0 | 0 | 100 | 0 |
| F | 100 | 0 | 0 | 29.8 | 60.2 | 0 | 15.7 | 84.3 | 0 | 0 | 100 | 0 |

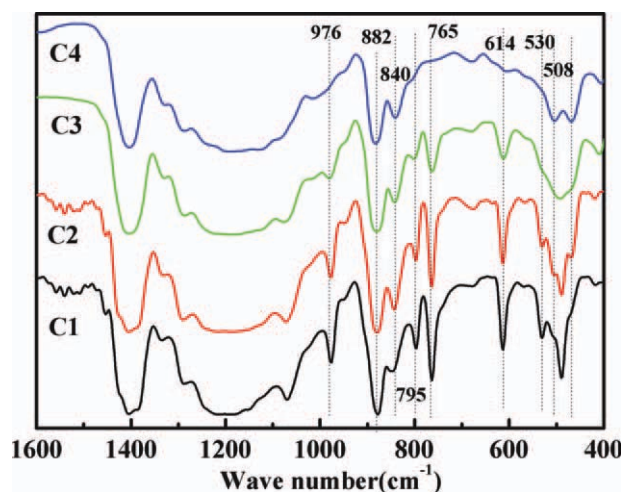


Figure 7. Infrared spectra of annealed P(VDF-*co*-TrFE) films containing different TrFE content: C1: 6 mol % TrFE; C2: 9 mol % TrFE; C3: 12 mol % TrFE; C4: 20 mol % TrFE. [Color figure can be viewed in the online issue, which is available at wileyonlinelibrary.com.]

are turned from $\alpha+\gamma$ phase (6 mol %) to $\alpha+\beta+\gamma$ phase (9 and 12 mol %) and eventually to neat β phase in copolymer containing 20 mol % TrFE. This trend could be more precisely obtained from the percentage calculation of each crystal phases listed in Table II. When TrFE content is as low as 6 mol %, the crystalline region is composed of large amount of α phase with minor content of γ phase. As TrFE content increases, the amount of β phase increases dramatically while that of α phase decreases greatly. Similar trends could be observed in the B, D, E, and F types of samples fabricated at high temperature followed by cooling at different rate. That means high fabrication temperature favors the formation of α phase for its highest thermodynamic stability unless sufficient TrFE units with steric bulk reinforce them to form *trans* conformation. However, the phase

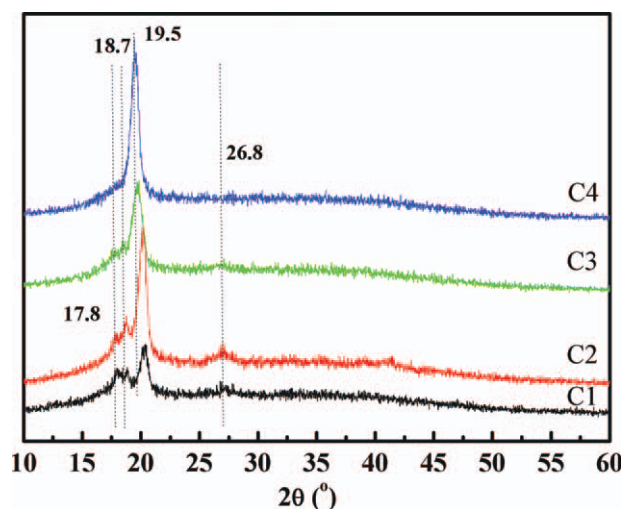


Figure 8. X-ray diffraction spectra of annealed P(VDF-*co*-TrFE) films containing different TrFE content: C1: 6 mol % TrFE; C2: 9 mol % TrFE; C3: 12 mol % TrFE; C4: 20 mol % TrFE. [Color figure can be viewed in the online issue, which is available at wileyonlinelibrary.com.]

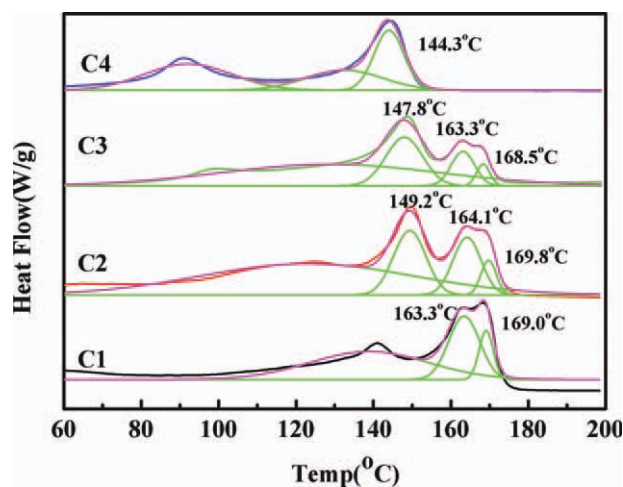


Figure 9. DSC of annealed P(VDF-*co*-TrFE) films containing various TrFE content. C1: 6 mol % TrFE; C2: 9 mol % TrFE; C3: 12 mol % TrFE; C4: 20 mol % TrFE. The inner curves (color in black, dark yellow, blue, dark cyan) come from the original measured data. The magenta curves represent the fitting lines while the green ones correspond to the separation results. [Color figure can be viewed in the online issue, which is available at wileyonlinelibrary.com.]

transition induced by TrFE addition is in a rather different way from $\alpha + \gamma$ phase (6 mol %) to $\beta+\gamma$ phase (9 mol %) and to neat β phase in copolymer containing 20 mol % TrFE as shown in Table II if the films are fabricated at low temperature (44°C). Apparently, the conclusion coincides very well with that obtained in neat PVDF, namely, films fabricated from solution cast in high polarity solvents (such as DMF, DMAc, and acetone) at low temperature favors the formation of γ phase while those fabricated at high temperature would result in the formation of α phase. The addition of TrFE is responsible for the formation of all-*trans* conformation (β phase) as well as part of the TTTG conformation (γ phase). The phase transition in indirect P(VDF-*co*-TrFE) with TrFE content less than 20 mol % could be attributed to the combined influence of fabrication conditions and addition of TrFE. Interestingly, the lowest TrFE molar content (about 20 mol %) for fabricating stable β phase in indirectly polymerized P(VDF-*co*-TrFE) is much lower than that of in directly polymerized P(VDF-*co*-TrFE). That may be attributed to the different VDF/TrFE connection sequence as described in literature,³⁹ which would be discussed in other work.

CONCLUSIONS

Three types of crystalline phase (α , β , and γ) of indirectly polymerized P(VDF-*co*-TrFE) have been well distinguished by employing FTIR, XRD, and DSC multiplex fitting techniques. α phase could be easily identified from the absorption bands at 530, 614, 764, 796, and 975 cm^{-1} on IR spectra and the diffraction reflection at $2\theta = 17.7^\circ$ and 26.8° on XRD. β and γ phases can be distinguished by DSC for their different melting temperature. Both the fabrication temperature and TrFE content are responsible for the phase transition of P(VDF-*co*-TrFE). Low temperature favors the formation of γ phase while those

fabricated at high temperature would result in the formation of α phase. The addition of TrFE is responsible for the formation of all-*trans* conformation (β phase) as well as part of the TTTG conformation (γ phase).

ACKNOWLEDGMENTS

This work was financially supported by National Nature Science Foundation of China-NSAF (Grant No. 50903065, 51103115, and 10976022), Fundamental Research Funds for the Central Universities, and International Science & Technology Cooperation Program of China (Grant No. 2010DFR50480). Qiuping Zhang is responsible for data acquisition and analysis work as well as the drafting work of this manuscript. Weimin Xia takes charge of the fabrication work of P(VDF-*co*-TrFE)s films while Zhigang Zhu is responsible for the preparation work of P(VDF-*co*-TrFE)s materials. Zhicheng Zhang instructs all the mentioned work as well as revising this manuscript.

REFERENCES

1. Kawai, H. *Japan J. Appl. Phys.* **1969**, *8*, 975.
2. Bergman, J. G., Jr.; McFec, J. H.; Grane, G. R. *Appl. Phys. Lett.* **1971**, *18*, 203.
3. Higashihata, Y.; Sako, J.; Yagi, T. *Ferroelectrics* **1981**, *32*, 85..
4. Yagi, T.; Higashihata, Y.; Fukuyama, K.; Sako, J. *Ferroelectrics* **1984**, *57*, 327.
5. Wang, T. T.; Herbert, J. M.; Glass, A. M., Eds. *The Application of Ferroelectric Polymers*; Blackie & Son: Glasgow, **1988**.
6. Tajitsu, Y.; Chiba, A.; Furukawa, T.; Date, M.; Fukada, E. *Appl. Phys. Lett.* **1980**, *36*, 286.
7. Yamada, T.; Ueda, T.; Kitayama, T. *J. Appl. Phys.* **1981**, *52*, 948.
8. Yamada, T.; Kitayama, T. *J. Appl. Phys.* **1981**, *52*, 6859.
9. Tashiro, K.; Takano, K.; Kobayashi, M.; Chatani, Y.; Tado-koro, H. *Polymer* **1981**, *22*, 1312.
10. Tashiro, K.; Takano, K.; Kobayashi, M.; Chatani, Y.; Tado-koro, H. *Polymer* **1984**, *25*, 195.
11. Tashiro, K.; Takano, K.; Kobayashi, M.; Chatani, Y.; Tado-koro, H. *Ferroelectrics* **1984**, *57*, 297.
12. Lovinger, A. J.; Furukawa, T.; Davis, G. T.; Broadhurst, M. G. *Polymer* **1983**, *24*, 1225.
13. Lovinger, A. J.; Furukawa, T.; Davis, G. T.; Broadhurst, M. G. *Polymer* **1983**, *24*, 1233.
14. Davis, G. T.; McKinney, J. E.; Broadhurst, M. G.; Roth, S. C. *J. Appl. Phys.* **1987**, *49*, 4998.
15. Yang, D. C.; Thomas, E. L. *J. Mater. Sci. Lett.* **1984**, *3*, 929.
16. Yang, D. C.; Chen, Y. J. *Mater. Sci. Lett.* **1987**, *6*, 599.
17. Koga, K.; Ohigashi, H. *J. Appl. Phys.* **1986**, *59*, 2142.
18. Yagi, T. *Polym. J.* **1979**, *11*, 353.
19. Yagi, T. *Polym. J.* **1979**, *11*, 711.
20. Yagi, T.; Tatemoto, M. *Polym. J.* **1979**, *11*, 429.
21. Yagi, T.; Tatemoto, M.; Sako, J. *Polym. J.* **1980**, *12*, 209.
22. Tanaka, R.; Tashiro, K.; Kobayashi, M. *Polymer* **1999**, *40*, 3855.
23. Barique, M. A.; Ohigashi, H. *Polymer* **2001**, *42*, 4981.
24. Kim, K. J.; Shaw, H. L. *Polymer* **1994**, *35*, 3612.
25. Neri, A.; Ruiz, P. R. O.; Job, A. E.; Oliveira, O. N. Jr.; Giacometti, J. A. *10th International Symposium on Electrets*, **1999**, 347.
26. Koga, K.; Nakano, N.; Hatton, T.; Ohigashi, H. *J. Appl. Phys.* **1990**, *67*, 965.
27. Lovinger, A. J. *Science* **1983**, *220*, 1115.
28. Lovinger, A. J.; Furukawa, T.; Davis, G. T.; Broadhurst, M. G. *Macromolecules* **1982**, *15*, 324.
29. Tashiro, K.; Kobayashi, M. *Polymer* **1988**, *29*, 426.
30. Tashiro, K.; Tanaka, R.; Ushitora, K.; Kobayashi, M. *Ferroelectrics* **1995**, *171*, 145.
31. Kim, K. J.; Nicholas, M. R.; Shaw, H. L. *Macromolecules* **1989**, *22*, 4395.
32. Gregorio, R., Jr.; Botta, M. M. *J. Polym. Sci. Part B: Polym. Phys.* **1998**, *36*, 403.
33. Prest, W. M., Jr.; Luca, D. J. *J. Appl. Phys.* **1978**, *49*, 5042.
34. Li, G. R.; Kagami, N.; Ohigashi, H. *J. Appl. Phys.* **1992**, *72*, 1056.
35. Tanaka, H.; Yukawa, H.; Nishi, T. *Macromolecules* **1988**, *21*, 2469.
36. Hulburt, J. D.; Feiring, A. E. *Chem. Eng. News* **1997**, *75*, 6.
37. Wang, Z. M.; Zhang, Z. C.; Mike Chung, T. C. *Macromolecules* **2006**, *39*, 4268.
38. Lu, Y. Y.; Claude, J.; Neese, B.; Zhang, Q. M.; Wang, Q. J. *Am. Chem. Soc.* **2006**, *128*, 8120.
39. Lu, Y. Y.; Claude, J.; Zhang, Q. M.; Wang, Q. *Macromolecules* **2006**, *39*, 6962.
40. Tan, S. B.; Liu, E. Q.; Zhang, Q. P.; Zhang, Z. C. *Chem. Commun.* **2011**, *47*, 4544.
41. Zhang, Z. C.; Meng, Q. J.; Mike Chung, T. C. *Polymer* **2009**, *50*, 707.
42. Fernandez, M. V.; Suzki, A.; Chiba, A. *Macromolecules* **1987**, *20*, 1806.
43. Cheng, Z. Y.; Bharti, V.; Xu, T. B.; Wang, S. X.; Zhang, Q. M.; Ramotowski, T.; Tito, F.; Ting, R. J. *Appl. Phys.* **1999**, *86*, 2208.
44. Li, W. J.; Meng, Q. J.; Zheng, Y. S.; Zhang, Z. C. *Appl. Phys. Lett.* **2010**, *96*, 192905.
45. Kim, K. J.; Kim, G. B. *Polymer* **1997**, *38*, 4881.
46. Li, W. P.; Yu, L. J.; Zhu, Y. J.; Hua, D. Y.; Wang, J.; Luo, H. L.; Zhang, J. J. *Appl. Polym. Sci.* **2010**, *116*, 663.
47. Stack, G. M.; Ting, R. Y. *J. Polym. Sci. Part B: Polym. Phys.* **1988**, *26*, 55.
48. Farmer, B. L.; Hopfinger, A. J.; Lando, J. B. *Appl. Phys.* **1972**, *43*, 4293.
49. Gregorio, R., Jr.; Cestari, M. J. *Polym. Sci. Part B: Polym. Phys.* **1994**, *32*, 859.